GEOPHYSICAL RESEARCH LETTERS, VOL. 34, L18705, doi:10.1029/2007GL031460, 2007

Click Here for Full Article

Large discrepancy between observed and simulated precipitation trends in the ascending and descending branches of the tropical circulation

Richard P. Allan[1] and Brian J. Soden[2]

Received 25 July 2007; revised 14 August 2007; accepted 22 August 2007; published 26 September 2007.

[1] Observed and model simulated changes in precipitation are examined using vertical motion at 500 hPa to define ascending and descending branches of the tropical circulation. Vertical motion fields from reanalyses were employed to subsample the observed precipitation data. An emerging signal of rising precipitation trends in the ascending regions and decreasing trends in the descending regimes are detected in the observational datasets. These trends are substantially larger in magnitude than present-day model simulations and projections into the 21st century. The discrepancy cannot be explained by changes in the reanalysis fields used to subsample the observations but instead must relate to errors in the satellite data or in the model parametrizations. This has important implications for future predictions of climate change, the reliability of the observing system and the monitoring of the global water cycle. **Citation:** Allan, R. P., and B. J. Soden (2007), Large discrepancy between observed and simulated precipitation trends in the ascending and descending branches of the tropical circulation, *Geophys. Res. Lett.*, *34*, L18705, doi:10.1029/2007GL031460.

1. Introduction

[2] Past changes in precipitation are thought to have profoundly affected past human societies [e.g., *Yancheva et al.*, 2007] and projected increases in the total area affected by drought and the flood risk associated with increased frequency of heavy precipitation events are expected to exert an adverse effect on agriculture, water resources, human health and infrastructure [*Meehl et al.*, 2007; *Kundzewicz et al.*, 2007]. Changes in atmospheric circulation patterns and in thermodynamic properties of the circulation regimes will dictate future regional precipitation changes [e.g., *Emori and Brown*, 2005]; in planning for and adapting to such changes, it is important to be able to predict this response accurately.

[3] There is a robust physical argument for changes in the character of precipitation in a warming world [e.g., *Trenberth et al.*, 2003; *Allen and Ingram*, 2002]. Convection typically draws moisture in from around 3–5 times the radius of the precipitating region [e.g., *Trenberth et al.*, 2003] and observational, modeling and theoretical studies suggest that atmospheric moisture will increase with warming at the rate of approximately 7% K^{-1}, primarily due to the Clausius Clapeyron relationship between saturated vapor pressure and temperature [e.g., *Soden et al.*, 2005]. This suggests that precipitation from convective systems will increase at a similar rate [e.g., *Trenberth et al.*, 2003; *Allen and Ingram*, 2002].

[4] Global mean precipitation is however constrained by the energy balance of the atmosphere. Models and observations suggest that atmospheric net radiative cooling (Q) will enhance with planetary warming, primarily due to increased thermal emission of a warmer atmosphere, at a rate of $\sim$3 $Wm^{-2}K^{-1}$ [e.g., *Allen and Ingram*, 2002; *Allan*, 2006]. Assuming a negligible change in sensible heat transfer between the surface and the atmosphere, this suggests that precipitation (P) will vary with surface temperature, T_s, as:

$$\frac{dP}{dT_s} \sim \frac{1}{\rho_w L}\frac{dQ}{dT_s}, \tag{1}$$

which is $\sim$0.1 mm day^{-1} K^{-1} or 3–4% K^{-1} (ρ_w is water density and $L = 2.5 \times 10^6$ Jkg^{-1}). Since this response is smaller than the expected convective region response, this implies that non-convective regions will experience reduced precipitation leading to greater extremes (more intense rainfall and longer dry spells [e.g., *Emori and Brown*, 2005] and enhanced seasonality [e.g., *Chou et al.*, 2007]).

[5] Modeling studies seem to conform to this argument, with global precipitation increasing at just 1–3% K^{-1} and evidence of drying in regions of net moisture divergence, in particular for regions at the periphery of convection [e.g., *Neelin et al.*, 2006; *Seager et al.*, 2007; *Meehl et al.*, 2005; *Wang and Lau*, 2006]. Anthropogenic influence on precipitation changes over land has been detected over broad latitudinal bands for the period 1925–1999 [*Zhang et al.*, 2007] although observed trends and variability are larger than climate model simulations. Satellite data also suggests that models underestimate the observed global precipitation response ($\sim$6% K^{-1}) which is close to the Clausius Clapeyron rate [*Wentz et al.*, 2007]. They further note that changes in precipitation lower than this rate would necessitate a reduction in global wind speed which is at odds with satellite observations over the oceans [*Yu and Weller*, 2007] but in agreement with measurements of wind speed and pan evaporation over land [*Roderick et al.*, 2007].

[6] Identifying regional trends in precipitation and their links with temperature and water vapor are problematic since local changes in these variables are particularly sensitive to subtle changes in the large-scale atmospheric circulation [e.g., *Zveryaev and Allan*, 2005]. To circumvent

[1]Environmental Systems Science Centre, University of Reading, Reading, UK.
[2]Rosenstiel School of Marine and Atmospheric Sciences, University of Miami, Miami, Florida, USA.

Copyright 2007 by the American Geophysical Union.
0094-8276/07/2007GL031460$05.00

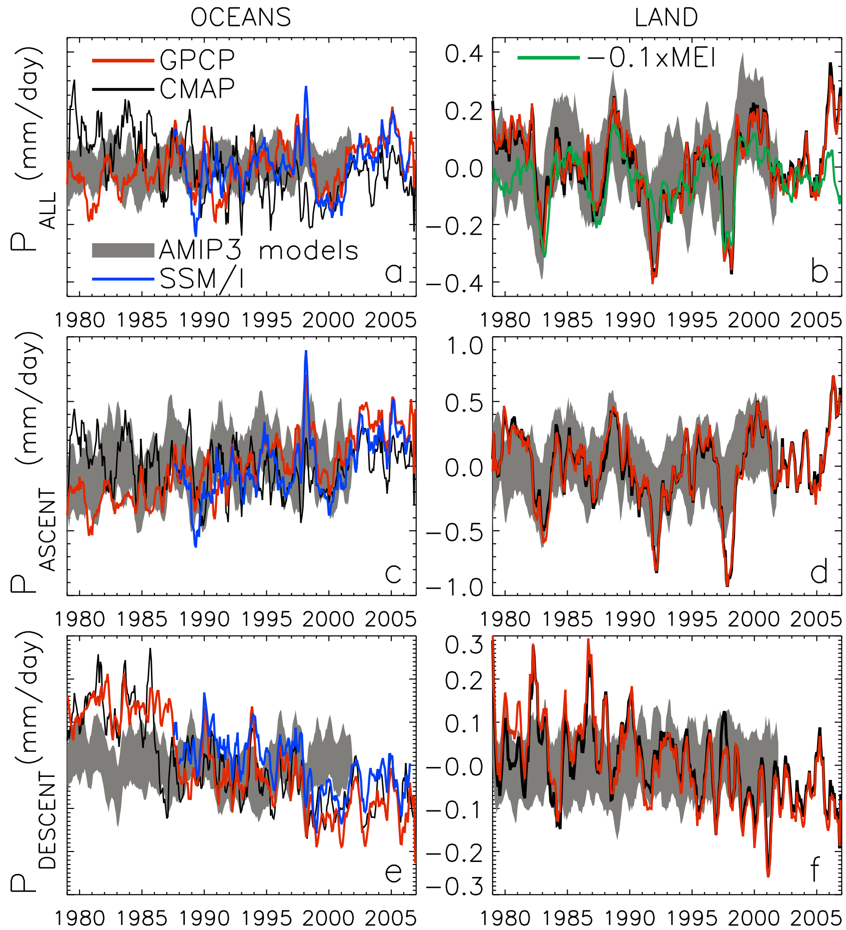

Figure 1. Deseasonalised changes in precipitation (mm day^{-1}) for observations and AMIP3 models for (a, b) the tropics (30°S–30°N) and regions of mean (c, d) ascent and (e, f) descent over land and ocean. A 5-month moving box-average was applied. Gray shading denotes the model ensemble mean ±1 standard deviation. Also shown in Figure 1b is the Multivariate ENSO Index (MEI) [*Wolter and Timlin*, 1998] multiplied by −0.1.

this issue, and to understand the nature of the discrepancy between observed and simulated precipitation changes, we seek in the present analysis to quantify the observed trends in precipitation within ascending and descending branches of the tropical circulation and compare with current model simulations of the present day and projections of future changes.

2. Data and Method

[7] Monthly mean precipitation from the Global Precipitation Climatology Project (GPCP) [*Adler et al.*, 2003] and from the Climate Prediction Center Merged Analysis of Precipitation (CMAP) [*Xie and Arkin*, 1998] enhanced product (V703) were employed for the period 1979–2006. Monthly mean intercalibrated precipitation from Version 6 Special Sensor Microwave Imager (SSM/I) data, described by *Wentz et al.* [2007], was used for the period 1987–2006.

[8] Simulations from the atmospheric components of an ensemble of models (CNRM_CM3, GISS_E_R, IAP_FGOALS, INMCM3, IPSL_CM4, MIROC_hires, MIROC_medres, MRI_CGCM2, NCAR_CCSM3, NCAR_PCM1, HadGEM1) forced with observed sea surface temperature over the period 1979–2001 (AMIP3) were extracted from the World Climate Research Programme (WCRP) model archive at the Program for Climate Model Diagnosis and Intercomparison (PCMDI) archive (www-pcmdi.llnl.gov). The AMIP3 model fields and the observed values were bi-linearly interpolated to a common 2.5 × 2.5° latitude-longitude grid.

[9] Coupled model simulations from the Climate of the 20th Century runs (1950–1999) and from the SRESA1B (stabilization at 720ppm CO_2 concentration) scenario (2000–2100) were analyzed using a model ensemble: CCCMA, CNRM_CM3, GFDL_CM2.1, GFDL_CM2.0, GISS_AOM, GISS_E_H, GISS_E_R, IAP_FGOALS, INMCM3, IPSL_CM4, MIROC_medres. These models were set up from control simulations and used prescribed natural and anthropogenic forcings [*Held and Soden*, 2006; *Emori and Brown*, 2005; *Meehl et al.*, 2005; *Wang and Lau*, 2006] (for a description of the model data, see www-pcmdi.llnl.gov).

[10] Area-weighted averages of the observed and simulated monthly mean fields were calculated for the tropics (30°S–30°N) and for the land-only and ocean-only regions. Additionally, vertical motion at 500 hPa (ω_{500}) was used to subsample regions of mean monthly ascending or descending motion. For the observations, ω_{500} was diagnosed from the National Center for Environmental Prediction/National

Table 1. Linear Trends and Standard Error for Deseasonalised Monthly Mean Precipitation, 1979–2006[a]

Dataset	Land + Ocean	Ocean	Land
		Tropics	
GPCP	0.032 ± 0.006*	0.044 ± 0.009*	−0.003 ± 0.013
CMAP	−0.052 ± 0.009*	−0.073 ± 0.012*	0.009 ± 0.013
SSM/I		0.039 ± 0.017*	
models	0.014 ± 0.003*	0.011 ± 0.004	0.024 ± 0.010
		Tropical Ascent	
GPCP	0.184 ± 0.014*	0.248 ± 0.019*	0.022 ± 0.026
CMAP	−0.023 ± 0.020	−0.027 ± 0.025	0.017 ± 0.026
SSM/I		0.243 ± 0.042*	
models	0.059 ± 0.011*	0.0110 ± 0.004	0.0237 ± 0.010
		Tropical Descent	
GPCP	−0.102 ± 0.005*	−0.111 ± 0.006*	−0.080 ± 0.008*
CMAP	−0.080 ± 0.006*	−0.092 ± 0.008*	−0.053 ± 0.008*
SSM/I		−0.072 ± 0.011*	
models	−0.006 ± 0.003	−0.008 ± 0.004	−0.001 ± 0.003

[a] *dP*/*dt* (mm day^{-1} decade^{-1}). Asterisk denotes significant correlation at the 99% level, allowing for autocorrelation. SSM/I, 1987–2006 period; ensemble mean of the AMIP3 models for the period, 1979–2001.

Center for Atmospheric Research reanalysis 1 (NCEP) [*Kalnay et al.*, 1996] for 1979–2006, or from the European Centre for Medium Range Weather Forecasts 40-year reanalysis (ERA40) [*Uppala et al.*, 2005] for 1979–2001.

3. Interannual Variability

[11] Variability of monthly mean precipitation is displayed in Figure 1. Observed variability is larger than the model envelope with substantial differences between CMAP and GPCP over the ocean (Figure 1a). Variability over land is consistent and related to the large-scale circulation response to El Niño Southern Oscillation (ENSO) as indicated by the close correspondence with the Multivariate ENSO Index (Figure 1b). The ocean-only SSM/I retrieval generally agrees with the GPCP record but there is a negative trend in the CMAP data, reported previously to relate to spurious use of atoll data and changes in the observing system [*Yin et al.*, 2004].

[12] Precipitation trends are computed in Table 1 for the observations and the ensemble mean of the AMIP3 models. Both observations and models include natural variability relating to ENSO although using an ensemble mean will smooth out some of the unforced natural variability compared to the observations. Despite this, a significant positive trend in the GPCP tropical mean data (0.03 mm day^{-1}dec^{-1}) is more than double the model ensemble mean trend, consistent with *Wentz et al.* [2007].

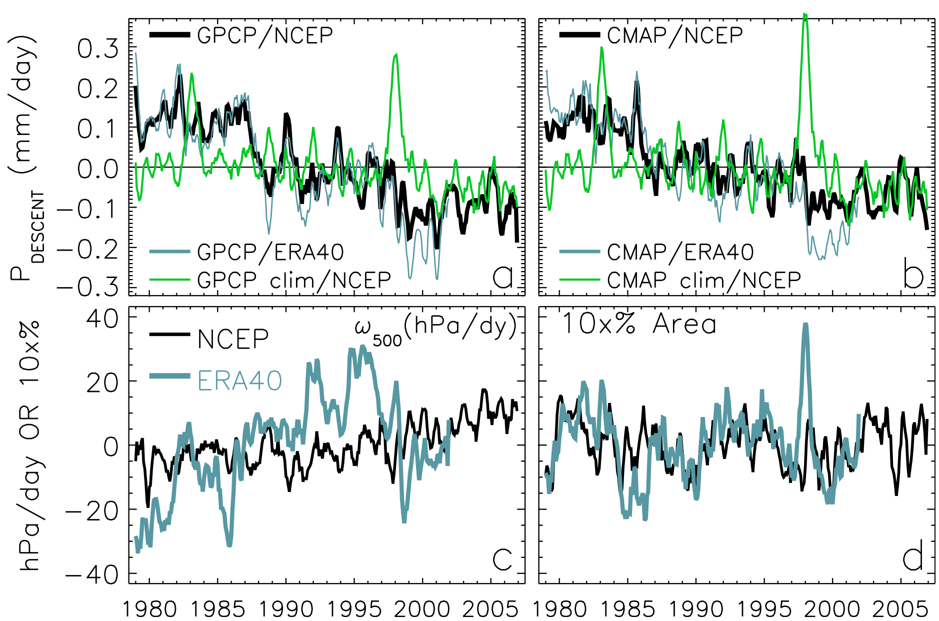

Figure 2. Deseasonalised changes in precipitation (*P*) over descent regions using NCEP vertical motion (ω_{500}) for (a) GPCP and (b) CMAP (black lines), including changes in *P* when ERA40 ω_{500} is applied (light blue), and where long-term climatologies of *P* are combined with the changing NCEP ω_{500} (green); changes in (c) ω_{500} and (d) areal extent of the descent region. A 5-month moving box-average was applied.

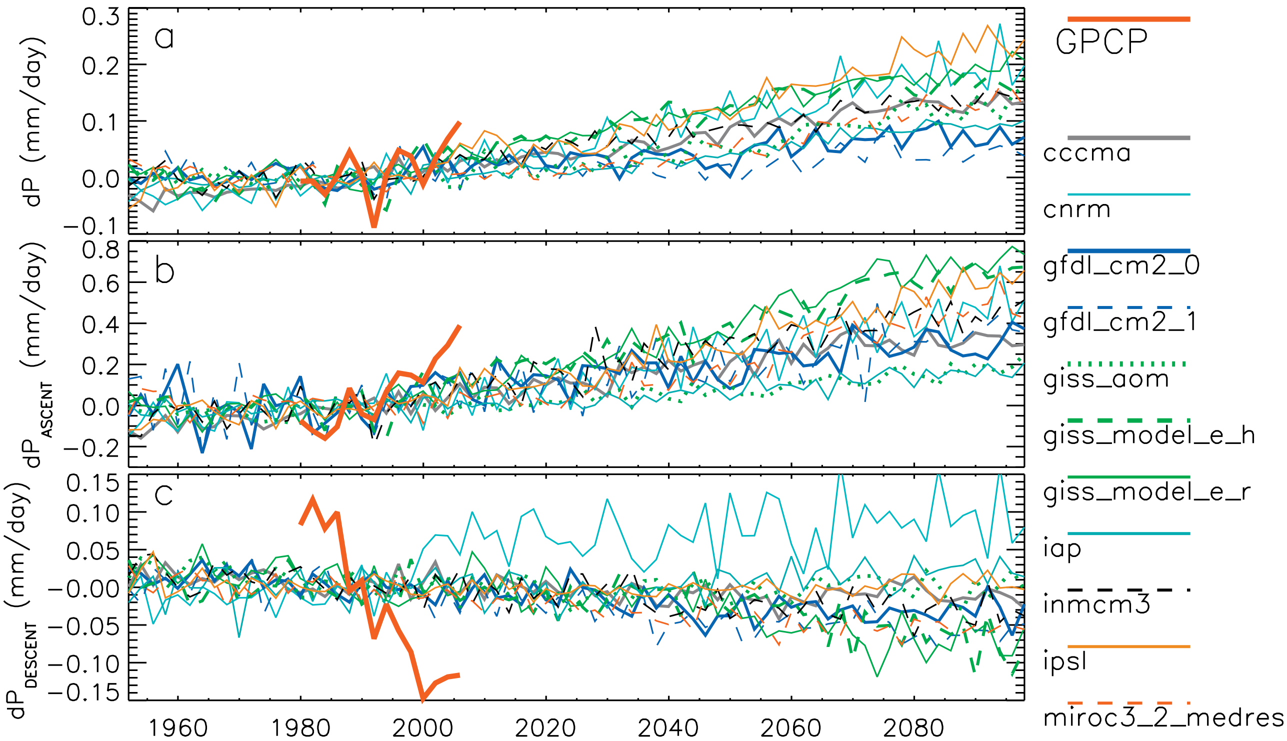

Figure 3. Tropical precipitation changes (mm day^{-1}), relative to 1979–2000, simulated by CMIP3 models over the period 1950–2100 for (a) all regions, (b) ascending regions, and (c) descending regions. Also shown are GPCP observed estimates. A 2-year average is applied to the model and observational data.

[13] Decomposing the tropical variability into ascending and descending regions produces more coherent trends in the data. For the ascending region of the tropical oceans (Figure 1c), an upward trend in P is evident in both GPCP and CMAP data from 1990–2006 with a similar trend for the SSM/I data. For the period 1979–1987, a large discrepancy between CMAP and GPCP data remains for the ocean region which affects the overall trends calculated in Table 1. An upward precipitation trend of 0.18 mm day^{-1} dec^{-1} in the GPCP data is substantially larger than the trend calculated for the entire tropics and a factor of 3 larger than the model ensemble mean trend.

[14] For the descending portions of the tropical circulation (Figures 1e and 1f) a coherent negative trend in observed precipitation is evident from all datasets over land and ocean (ranging from -0.05 to -0.11 mm day^{-1} dec^{-1}), but not detectable in the model simulations (Table 1).

4. Sensitivity to Observing System

[15] It is clear that the observed trends in precipitation are larger than the model simulations, in particular for the descending regions. It is important to assess whether this discrepancy may be explained by spurious changes in the reanalysis ω_{500} fields or in the satellite observing systems. Figures 2a and 2b show that for the descending regime, a negative precipitation trend is present for GPCP and CMAP using NCEP ω_{500} and the trend is larger still when using ERA40 ω_{500} (blue lines). Figures 2a and 2b also show the changes in precipitation calculated when applying the changing NCEP ω_{500} to a long-term monthly climatology of precipitation. Any detectable trend would relate to changes in the reanalysis fields rather than the precipitation estimates. A negative trend of around 0.025 mm day^{-1} decade^{-1} is calculated, less than 30% of the observational trends calculated in Table 1, although this is not significant at the 95% confidence level for the GPCP climatology. This suggests that the observed changes in P are sensitive to the reanalysis fields but that this cannot explain most of the precipitation responses found in the descending region.

[16] Figure 2c displays increasing descent-region ω_{500} (stronger descent) although with greater variability in ERA40 than NCEP. It is possible that these changes are artifacts of the observing system [*Held and Soden*, 2006] and these may contribute to a portion of the observed trends. Changes in the areal extent of the descending regime (Figure 2d) shows coherent variability in NCEP and ERA40 but no visible trend.

[17] We also examined the sensitivity of the observed trends to the products used. Using the GPCP gauge-only product (pg1–pg2) over land and the multi-satellite product (pms) over oceans produced trends within the statistical uncertainty of the standard GPCP product. The standard CMAP product (V705) produced trends that were within the statistical uncertainty of the enhanced product. Finally, when a simple merged average of all the SSM/I satellites was used, the negative trend over descending regions was enhanced by 30% while trends elsewhere were not statistically significant.

5. Long Term Projections

[18] Having established the robust nature of observed precipitation trends, we now place the variation in the

Table 2. Tropical Mean Precipitation and Linear Trends ±1 Standard Error for GPCP and CMIP3 Model Ensemble Means, 1979–2006[a]

Dataset	All	Ascent	Descent
		P (mm day^{-1})	
GPCP	2.9	5.0	1.1
models	3.5	6.4	1.4
		dP/dt (mm day^{-1}decade^{-1})	
GPCP	0.031 ± 0.013	0.183 ± 0.023*	−0.102 ± 0.011*
models	0.010 ± 0.003*	0.033 ± 0.010*	0.000 ± 0.002
models[b]	0.012 ± 0.0003*	0.037 ± 0.001*	−0.002 ± 0.0002*

[a]Asterisk denotes correlation >99% significance level.
[b]CMIP3 model ensemble mean for 1950–2100 period.

context of the longer term CMIP3 climate model projections. Figure 3 shows the tropical mean changes in P, relative to the reference period 1979–2000. The models generate natural variability, including ENSO-like behaviour, in addition to the longer time-scale trends in precipitation relating to the radiative forcing of climate. To reduce the impact of this unforced variability upon the calculation of trends, 2-year averaging is applied. The upward response of tropical precipitation in the models becomes increasingly clear in the 21st century; increases for the ascent region are ∼3 times larger than the tropical mean (Table 2) while for the descent region precipitation response is of variable sign but predominately reducing with time.

[19] GPCP displays a trend ∼5 times larger than the corresponding model ensemble mean trend over the ascending regions. Over descending regions, GPCP estimates show a large negative trend of −0.1 mm day^{-1}dec^{-1}. No trend is detected in the model data for the descending regimes over this period although a negative trend of just 0.002 mm day^{-1}dec^{-1} is calculated for the 1950–2100 period. Since GPCP mean P is lower than the model ensemble means, observed trends are even larger than the models when calculating percentage changes in P.

6. Discussion

[20] There is a large discrepancy between the observed and simulated precipitation changes over the tropics. A negative trend in CMAP data over the ascending-ocean region of the tropics before 1998 is thought to be spurious [e.g., *Yin et al.*, 2004]; for the remaining comparisons, robust upward trends in the ascending regime and downward trends in the descending portions of the tropical circulation are found in GPCP, CMAP and SSM/I datasets. For the tropics, the GPCP trend is about 2–3 times larger than the model ensemble mean trend, consistent with previous findings [*Wentz et al.*, 2007] and also supported by the analysis of *Yu and Weller* [2007] who argue that observed increases in evaporation over the ocean are substantially greater than those simulated by climate models. Are these changes in the atmospheric hydrological cycle plausible?

[21] Considering the tropical ocean ascent regions, for the period 1988–2006, the NCEP surface temperature trend is 0.15 ± 0.02 K dec^{-1}, within 1 standard error of the tropical mean trend. Analysing the SSM/I data over tropical ocean ascent regions, the precipitation mean (5.45 mm) and trend (0.257 ± 0.043 mm dec^{-1}) corresponds to a precipitation trend of 31% K^{-1}. The SSM/I column integrated water vapor mean (45.6 mm) and trend (0.96 ± 0.11 mm dec^{-1}) over the same domain results in an increase of 14% K^{-1}, slightly larger than the Clausius Clapeyron rate scaled by the moist adiabatic lapse rate factor (∼9% K^{-1} [*Wentz et al.*, 2007]), and around half the precipitation response. This implies enhanced moisture transport that is at odds with observations of a weakening tropical circulation [*Vecchi et al.*, 2006; *Wentz et al.*, 2007].

[22] One obvious explanation is that changes in the observing system and satellite calibration and retrieval errors introduce spurious variations. It is estimated that changes in the reanalysis vertical motion fields, that possibly relate to artificial trends in tropical temperature lapse rate in radiosonde data [*Held and Soden*, 2006], potentially explain up to one third of the trends in the descending region. Agreement between multiple datasets over this regime suggest the remaining changes are from the precipitation datasets although all products use SSM/I data from 1988 onwards and so are not independent; it is possible that satellite retrieval errors dependent on temperature or water column could explain these trends. However, a downward trend is also detectable over land-descent regions where rain-gauge data is utilized, suggesting that these changes are robust. Observed precipitation changes over land also appear larger than model simulations over the 20th century [*Zhang et al.*, 2007].

[23] An increase in global mean precipitation with temperature of around 6%K^{-1} [*Wentz et al.*, 2007] requires an increase in the atmospheric net radiative cooling that is larger than expected [*Allen and Ingram*, 2002]. It is possible that the models do not capture decadal variability in precipitation and radiative cooling adequately, possibly relating to changes in cloud and aerosol radiative effects [e.g., *Wielicki et al.*, 2002; *Mishchenko et al.*, 2007]. Continued monitoring of tropical precipitation and further improvements in satellite calibration and retrieval algorithms are required to explain the large discrepancy between observed and model predicted changes in the atmospheric hydrological cycle.

[24] **Acknowledgments.** Thanks to the WCRP for enabling the PCMDI model archive (www-pcmdi.llnl.gov). R. Allan was supported by NERC grant NE/C51785X/1. GPCP data were extracted from www.ncdc.noaa.gov and CMAP data from www.cdc.noaa.gov; SSM/I data were provided by Remote Sensing Systems. Thanks to V. John and G. Vecchi for useful discussion and to two anonymous reviewers who helped to improve the manuscript.

References

Adler, R. F., et al. (2003), The version-2 Global Precipitation Climatology Project (GPCP) monthly precipitation analysis (1979–present), *J. Hydrometeorol.*, *4*, 1147–1167.
Allan, R. P. (2006), Variability in clear-sky longwave radiative cooling of the atmosphere, *J. Geophys. Res.*, *111*, D22105, doi:10.1029/2006JD007304.
Allen, M. R., and W. J. Ingram (2002), Constraints on future changes in climate and the hydrologic cycle, *Nature*, *419*, 224–232.
Chou, C., J. Tu, and P. Tan (2007), Asymmetry of tropical precipitation change under global warming, *Geophys. Res. Lett.*, *34*, L17708, doi:10.1029/2007GL030327.
Emori, S., and S. J. Brown (2005), Dynamic and thermodynamic changes in mean and extreme precipitation under changed climate, *Geophys. Res. Lett.*, *32*, L17706, doi:10.1029/2005GL023272.
Held, I. M., and B. J. Soden (2006), Robust responses of the hydrological cycle to global warming, *J. Clim.*, *19*, 5686–5699.
Kalnay, E., et al. (1996), The NCEP/NCAR 40-year reanalysis project, *Bull. Am. Meteorol. Soc.*, *77*, 437–471.

Kundzewicz, Z. W., et al. (2007), Freshwater resources and their management, in *Climate Change 2007: Impacts, Adaptation and Vulnerability. Contribution of Working Group II to the Fourth Assessment Report of the Intergovernmental Panel on Climate Change*, edited by M. L. Parry et al., pp. 173–210, Cambridge Univ. Press, Cambridge, U. K.

Meehl, G. A., J. M. Arblaster, and C. Tebaldi (2005), Understanding future patterns of increased precipitation intensity in climate model simulations, *Geophys. Res. Lett.*, *32*, L18719, doi:10.1029/2005GL023680.

Meehl, G. A., et al. (2007), Global Climate Projections, in *Climate Change 2007: The Physical Science Basis. Contribution of Working Group I to the Fourth Assessment Report of the Intergovernmental Panel on Climate Change*, edited by S. Solomon et al., pp. 747–845, Cambridge Univ. Press, Cambridge, U. K.

Mishchenko, M. I., I. V. Geogdzhayev, W. B. Rossow, B. Cairns, B. E. Carlson, A. A. Lacis, L. Liu, and L. D. Travis (2007), Long-term satellite record reveals likely recent aerosol trend, *Science*, *315*, 1543.

Neelin, J. D., M. Munnich, H. Su, J. E. Meyerson, and C. E. Holloway (2006), Tropical drying trends in global warming models and observations, *Proc. Natl. Acad. Sci. U. S. A.*, *103*(16), 6110–6115.

Roderick, M. L., L. D. Rotstayn, G. Farquhar, and M. Hobbins (2007), On the attribution of changing pan evaporation, *Geophys. Res. Lett.*, *34*, L17403, doi:10.1029/2007GL031166.

Seager, R., et al. (2007), Model projections of an imminent transition to a more arid climate in southwestern North America, *Science*, *316*, 1181–1184.

Soden, B. J., D. L. Jackson, V. Ramaswamy, M. D. Schwarzkopf, and X. Huang (2005), The radiative signature of upper tropospheric moistening, *Science*, *310*, 841–844.

Trenberth, K. E., A. Dai, R. M. Rasmussen, and D. B. Parsons (2003), The changing character of precipitation, *Bull. Am. Meteorol. Soc.*, *84*, 1205–1217.

Uppala, S. M., et al. (2005), The ERA-40 re-analysis, *Q. J. R. Meteorol. Soc.*, *131*, 2961–3012.

Vecchi, G. A., B. J. Soden, A. T. Wittenberg, I. M. Held, A. Leetmaa, and M. J. Harrison (2006), Weakening of tropical Pacific atmospheric circulation due to anthropogenic forcing, *Nature*, *441*, 73–76.

Wang, H., and K. M. Lau (2006), Atmospheric hydrological cycle in the tropics in twentieth century coupled climate simulations, *Int. J. Climatol.*, *26*, 655–678.

Wentz, F. J., L. Ricciardulli, K. Hilburn, and C. Mears (2007), How much more rain will global warming bring?, *Science*, *317*, 233–235.

Wielicki, B. A., et al. (2002), Evidence for large decadal variability in the tropical mean radiative energy budget, *Science*, *295*, 841–844.

Wolter, K., and M. S. Timlin (1998), Measuring the strength of ENSO events: How does 1997/98 rank?, *Weather*, *53*, 315–324.

Xie, P., and P. A. Arkin (1998), Global monthly precipitation estimates from satellite-observed outgoing longwave radiation, *J. Clim.*, *11*, 137–164.

Yancheva, G., et al. (2007), Influence of the intertropical convergence zone on the east Asian monsoon, *Nature*, *445*, 74–77.

Yin, X., A. Gruber, and P. Arkin (2004), Comparison of the GPCP and CMAP merged gauge-satellite monthly precipitation products for the period 1979–2001, *J. Hydrometeorol.*, *5*, 1207–1222.

Yu, L., and R. A. Weller (2007), Objectively analyzed air-sea heat fluxes for the global ice-free oceans (1981–2005), *Bull. Am. Meteorol. Soc.*, *88*, 527–539.

Zhang, X., et al. (2007), Detection of human influence on twentieth-century precipitation trends, *Nature*, *448*, 461–465.

Zveryaev, I. I., and R. P. Allan (2005), Water vapor variability in the tropics and its links to dynamics and precipitation, *J. Geophys. Res.*, *110*, D21112, doi:10.1029/2005JD006033.

R. P. Allan, Environmental Systems Science Centre, University of Reading, Harry Pitt Building, Whiteknights, Reading, Berkshire RG6 6AL, UK. (rpa@mail.nerc-essc.ac.uk)

B. J. Soden, Rosenstiel School of Marine and Atmospheric Sciences, University of Miami, 4600 Rickenbacker Causeway, Miami, FL 33149, USA. (bsoden@rsmas.miami.edu)